Pulsed-Neutron Logging (PNL) for the GeoCquest Field Validation Project

Aman Raizada, Sally M. Benson

November 19, 2024

Stanford | Doerr School of Sustainability | Stanford Center for Carbon Storage

Agenda

- CO_2 Saturation Monitoring with Pulsar*
- Defining Logging Protocols
- Novel physics-based Method for Enhancement of Log Resolution
- Acquisition of Baseline PN-logs
- Acquisition of Monitoring logs
- Upcoming Milestones and Future Work

**Multifunction Spectroscopy device by SLB*

Example of Expected Saturation Changes in CRC-8

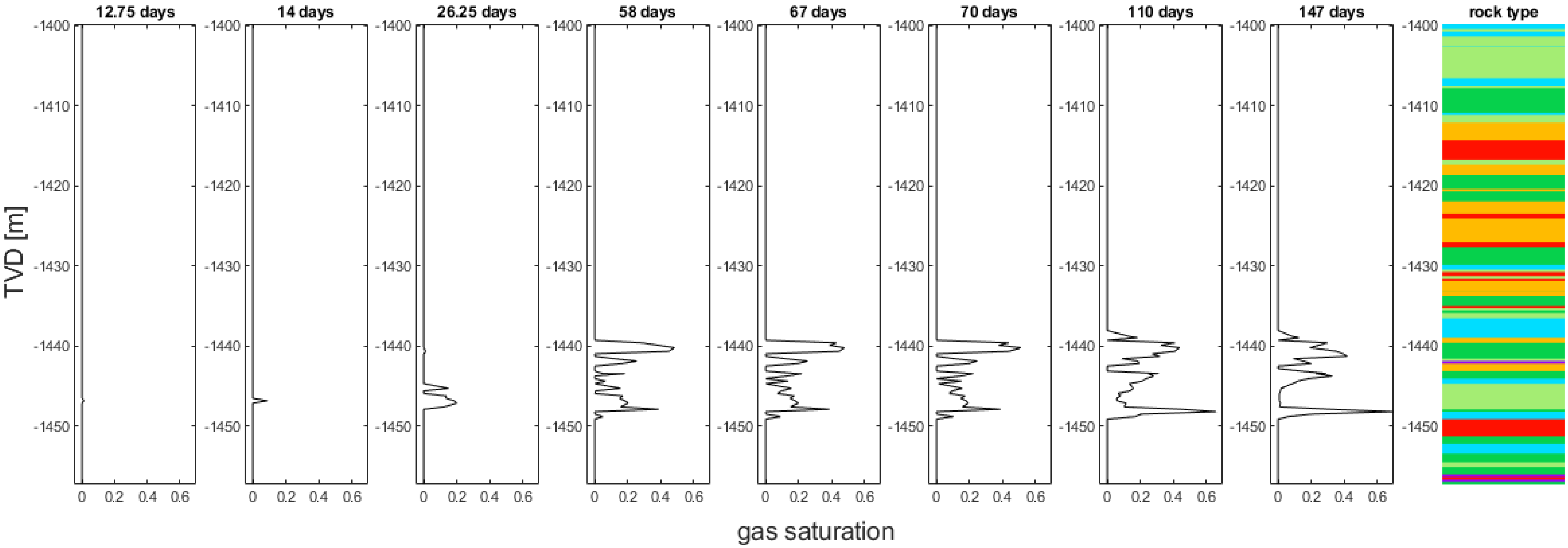

Saturation profiles simulated for one realization of a high-resolution dynamic reservoir simulation of the Paaratte-2 formation using GEOS with directional relative permeability curves

CO_2 Saturation Monitoring with Pulsar

Energy Spectroscopy (IC)

- Elemental concentrations
- Carbon/Oxygen
- TOC

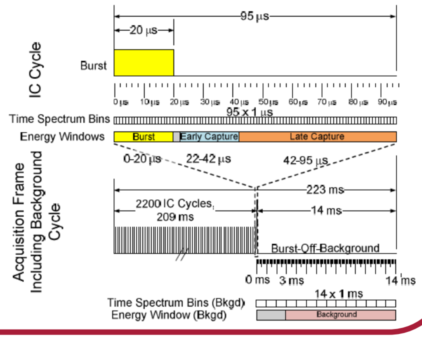

+

Time Spectrum (GSH)

- Hydrogen Index (H)
- Sigma (S)
- Inelastic Gas (G)

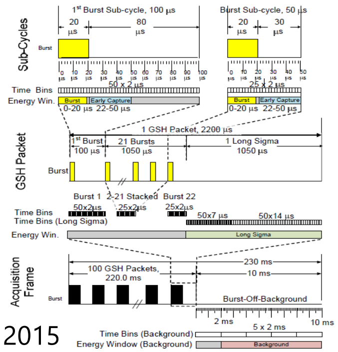

Source: Rose et al. 2015

=

Proposed Logging mode

GSH-Lithology

Comprehensive suite of measurements in a *single* pass

- FNXS
- SIGM
- Porosity
- Full Spectroscopy

Defining Logging Protocols

Plan for logging speed:

Logging runs in GSH-Lith mode at slow speed

- Utilize a low-speed gearbox allowing a logging speed of approximately 200 ft/hr
- Sampling rate of 0.5 ft

1800 ft/hr

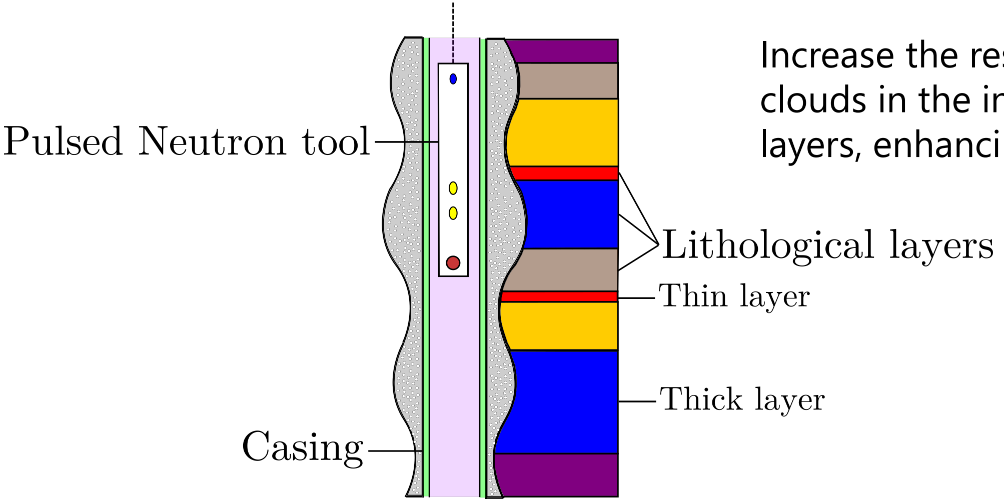

Increase the residence time of neutron clouds in the investigation volume across layers, enhancing precision

200 ft/hr

More Recommended Logging Protocols

Multiple baseline pre-injection pulsed-neutron logs

- Highly accurate pre-injection baseline logs are essential for detecting small changes in petrophysical quantities during time-lapse interpretation
- Open Hole (OH) and pre-injection baseline logs serve as crucial inputs for inversion of time-lapse logs

More Recommended Logging Protocols

Other useful protocols being followed:

- ❑ Maintaining consistent tension in the cable string
- ❑ Minimizing any acceleration in the cable velocity while logging over the monitoring interval
- ❑ Monitor changes, such as the formation of a sump in CRC-3, during well shut-in after injection
- ❑ Monitor local cooling around the perforated interval due to the Joule-Thompson effect during CO_2 injection (relevant for injection well logging)
- ❑ Specialized non-commercial algorithms from SLB will be used for data processing when CO_2 is present in the injector borehole (relevant for injection well logging)

Novel Physics-based Method for Enhancement of Log Resolution

Sliding-Window approach to enhance the resolution of PN-logs

- Data samples acquired by the tool come from overlapping volumes of investigation
- Idea is to deconvolute the effect of heterogeneous layers using the sliding window approach

$$Volume\ of\ investigation\ of\ the\ tool = Size\ of\ sliding\ window$$

$$Sampling\ interval = Distance\ moved\ by\ the\ sliding\ window$$

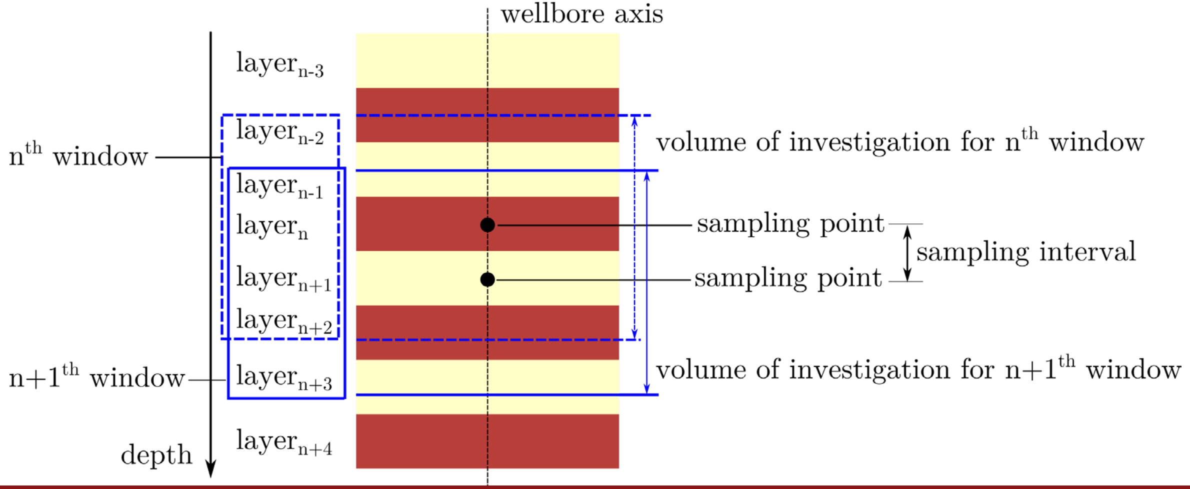

Step 1: Acquisition of low-resolution PN-logs

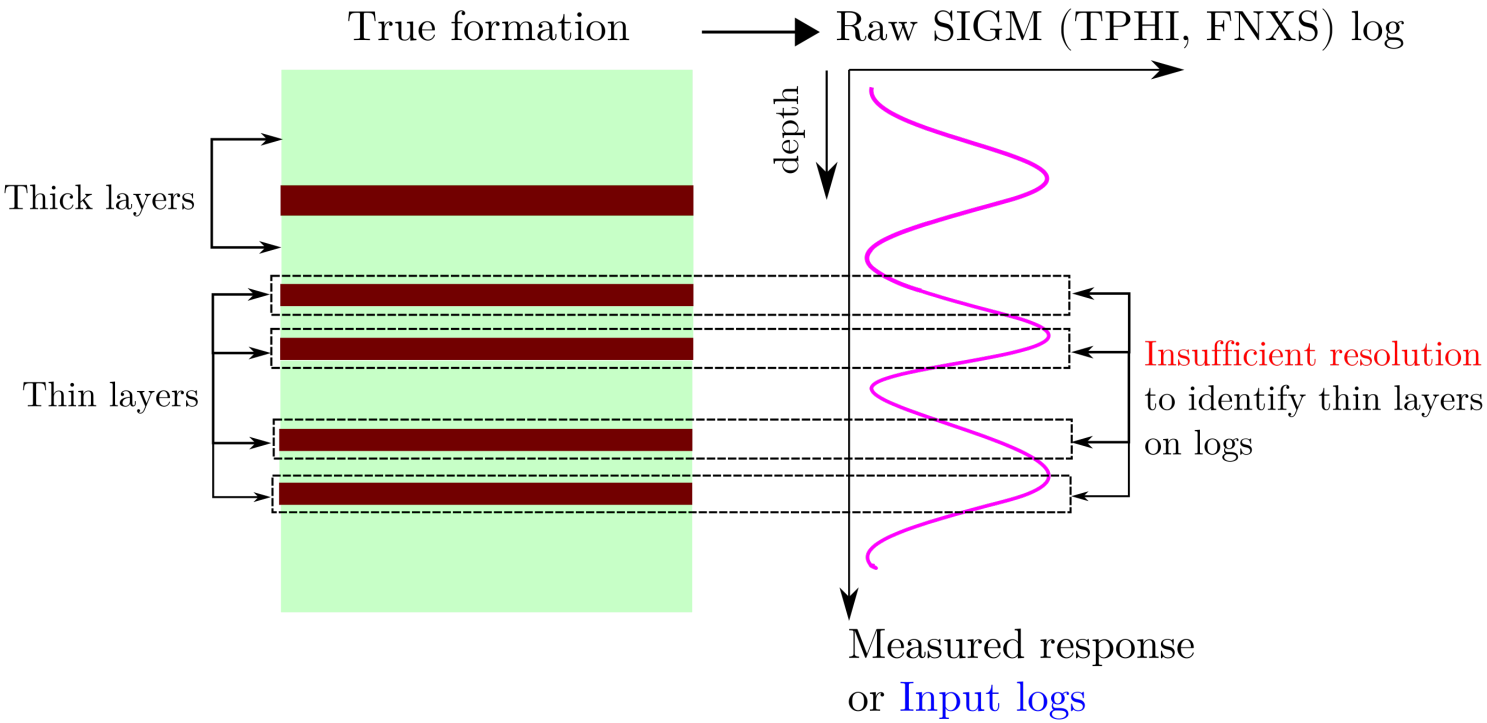

Step 2: Mathematical formulation of the target problem

Step 2(a): Defining the objective function

$$b(i) = \int_{z=i-\frac{1}{2}VR}^{i+\frac{1}{2}VR} w_{iz} \cdot x(z)\, dz \approx \sum_{z=i-\frac{1}{2}VR}^{i+\frac{1}{2}VR} w_{iz} \cdot x(z) \cdot \Delta z$$

$b(i)$ log values at sampled depth i

w_{iz} weight coefficients at sampled depth i over the depth of investigation

$x(z)$ real (or in-situ) properties of layer at depth z

VR vertical resolution of the PNL tool

Step 2(b): Physics-based constraints

Using the well-log interpretation model, the upper and lower bounds of measured properties, such as porosity, SIGM, etc., are computed interactively

Step 2(c): Deterministic optimization problem

$$x'_{high-res} = argmin_{high-res}(b(i) - sim(i))^2$$

$$given\ constraints$$

Algorithm: Constrained least squares method

Step 3: Data Assimilation

- The sliding window technique is employed to obtain a sufficient number of equations
- This method simulates the operating state of the tool, as the current tool sampling includes overlapping formation information from previous samplings

$(n-1)^{th}$ $window$

n^{th} $window$

$\cdots$ $Layer_{n-3}$ $Layer_{n-2}$ $Layer_{n-1}$ $Layer_{n}$ $Layer_{n+1}$ $Layer_{n+2}$ $Layer_{n+3}$ $\cdots$

depth

transform to equations

$$
\begin{array}{r}
\\
\\
\\
n^{th}\ window\ equation
\end{array}
\begin{bmatrix}
w_{11}x_1 + w_{12}x_2 + w_{13}x_3 + w_{14}x_4 + w_{15}x_5 \\
w_{22}x_2 + w_{23}x_3 + w_{24}x_4 + w_{25}x_5 + w_{26}x_6 \\
\cdots \\
w_{i(n-2)}x_{n-2} + w_{i(n-1)}x_{n-1} + w_{i(n)}x_n + w_{i(n+1)}x_{(n+1)} + w_{i(n+2)}x_{n+2} \\
\cdots
\end{bmatrix}
=
\begin{bmatrix}
b(3) \\
b(4) \\
\cdots \\
b(n) \\
\cdots
\end{bmatrix}
$$

Step 4: Output high-resolution PN-logs

- The solution to the optimization problem results in estimation of the true profile of the formation with enhanced resolution

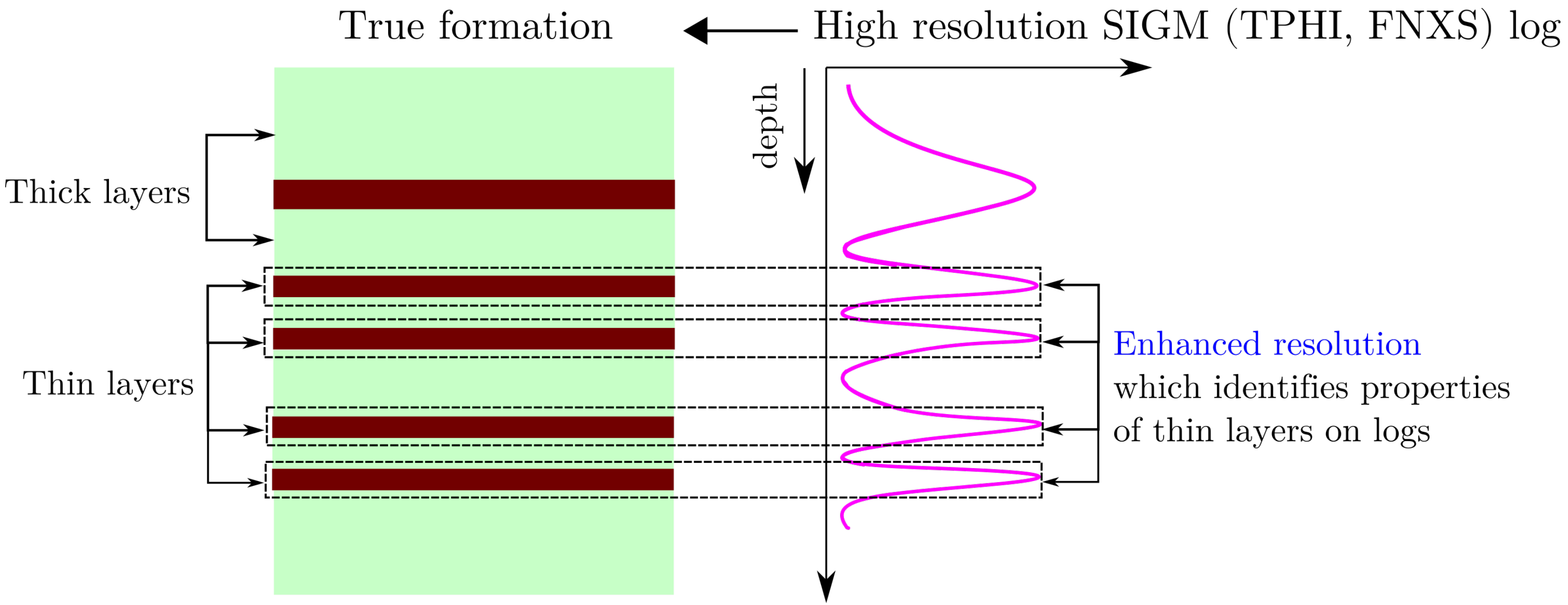

Application to synthetic logs

- An artificial Earth model is assumed to be made up of clay and sand lithologies
- The properties* of the model are defined as follows:

Thickness of high permeability layers (clean sand)	$\{91.44\ cm, 60.96\ cm, 30.48\ cm, 20\ cm, 15\ cm, 9\ cm\}$
Porosity of (high , low) permeability layers	$(0.5\ , 0.00001)$
CO2 saturation in (high , low) permeability layers	$(0.4\ , 0)$

- Synthetic logs are generated using the 1-D well log simulator at following operational inputs:

Logging speed	$200\ ft/hr$
Sampling interval (or rate)	$0.5\ ft$
Vertical resolution (VR) of PN-tool	$2.5\ ft^{+}$

* *Endpoints for Nuclear measurements obtained from Schlumberger NUclear PARameters (SNUPAR) code*
\+ *Typical log resolution of Pulsar after depth filtering (assumed to be same for all measurements for demonstration)*

Results from the application of the Algorithm

- Workflow tested on synthetic logs
- Provides a method to extract high-resolution information from raw Pulsed-Neutron logs
- Integrate with high-resolution logs, such as FMI, for higher accuracy

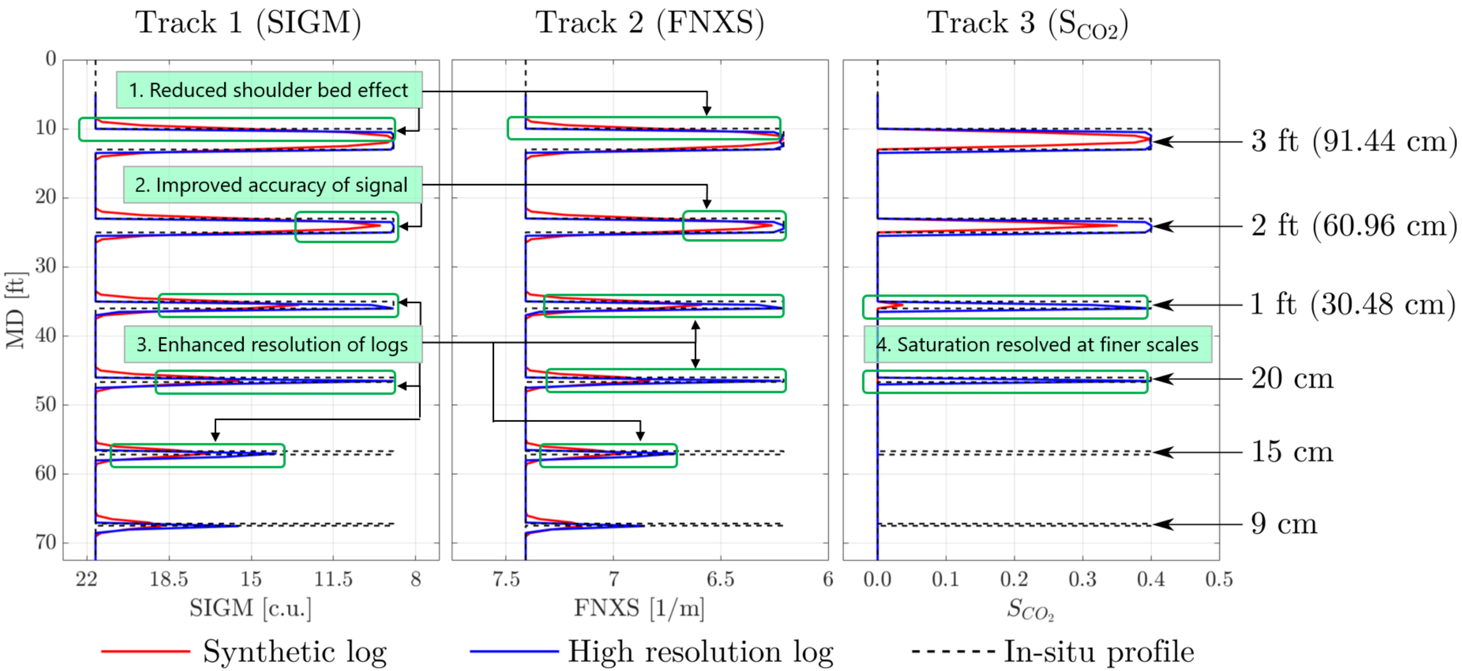

Acquisition of Baseline logs

4 passes of baseline logs have been acquired in:

- Eccentered configuration
- Centered configuration

The repeatability of the logs has been assessed to decide the configuration for monitoring logging runs

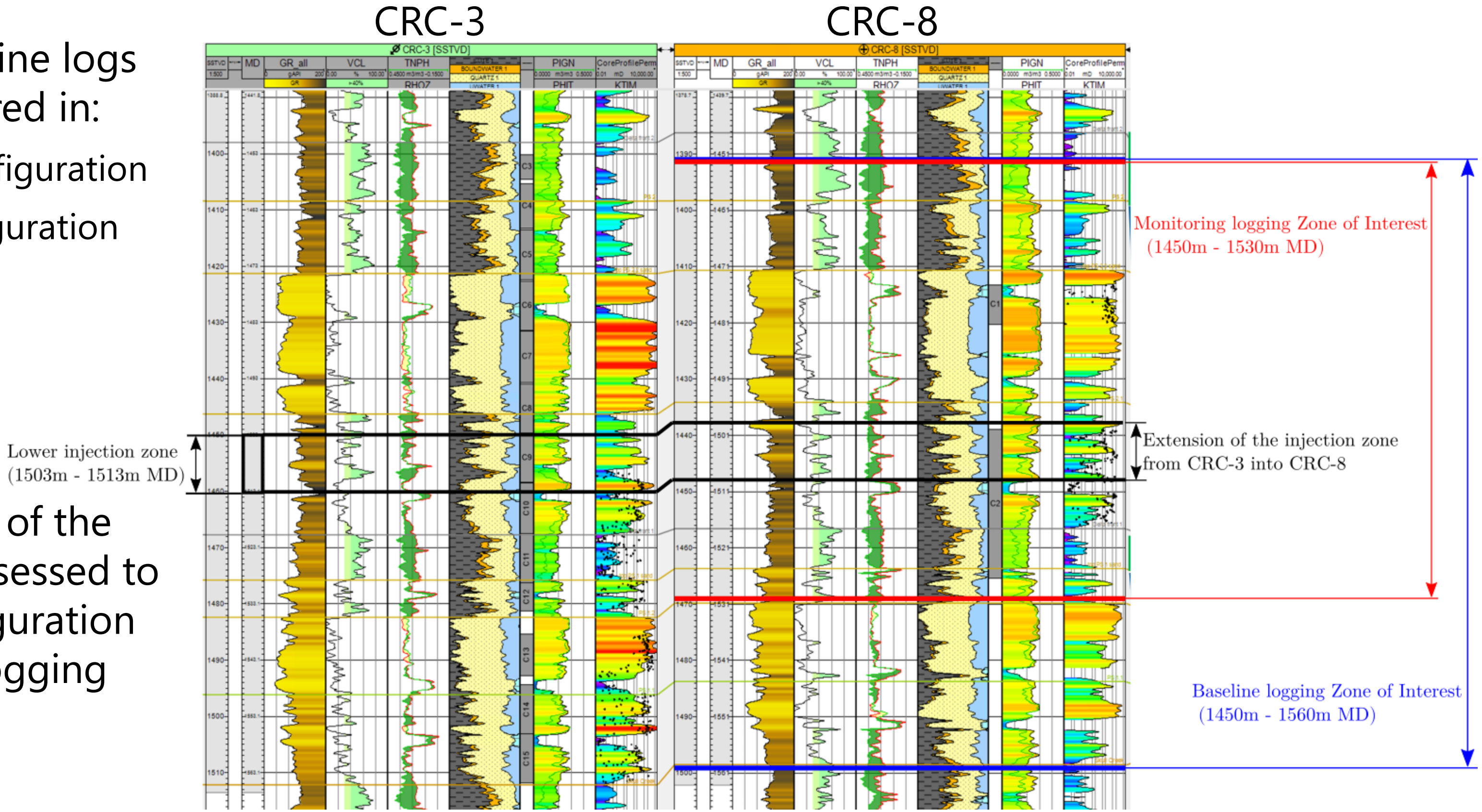

Baseline logs in CRC-8

Key observations:

- Good overlap between the Open-Hole TNPH log and the TPHI logs from the Eccentered configuration (Cased-Hole logs)
- TNPH logs used for accurate depth matching
- Both, SIGM and TPHI, being self-compensated measurements, show very good repeatability across all passes
- Mineralogical yields are accurate and consistent with OH-logs, with additional information about the presence of pyrite
- No gas was observed in the Zone of Interest (PS 2) during the baseline logging conducted in the pre-injection period

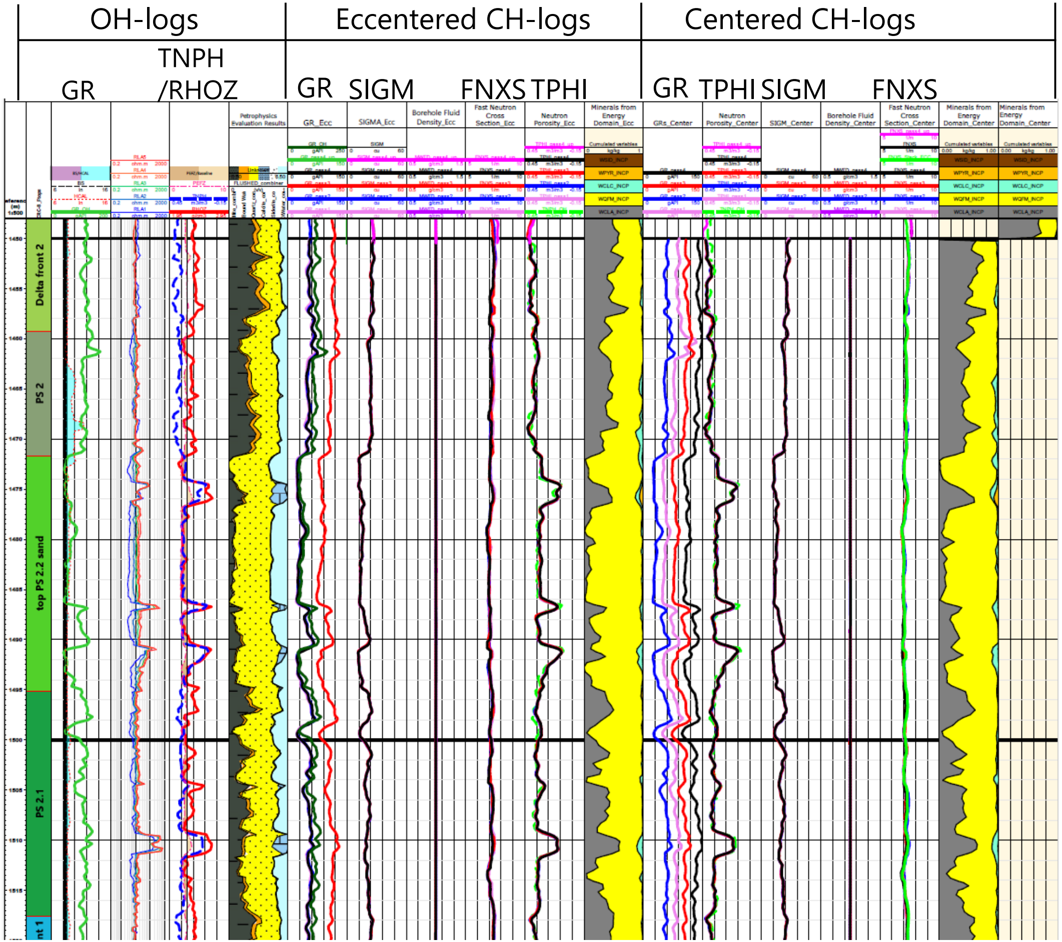

Quantifying PNL Repeatability

PNL precision: "Closeness of agreement between baseline PNL measurements and subsequent repeat PNL measurements from the same depth in CRC-8"

The Coefficient of Variation (CV) is used to assess the repeatability of PN-logs across multiple passes in different configurations at each sampling depth

$$CV = \frac{\sigma}{\mu} = \frac{standard\ deviation}{mean}$$

Repeatability of GSH-measurements

Key observations:

- Excellent repeatability observed for SIGM, FNXS, and TPHI across all passes, attributed to the slow logging speed (resulting in better radiation counting statistics)
- SIGM is the most robust measurement, followed by TPHI
- In comparison, FNXS is more susceptible to borehole effects due to its shallow depth of investigation (~3-4 inches)

Plots of GSH-measurements for the first pass in the eccentralized configuration for baseline run

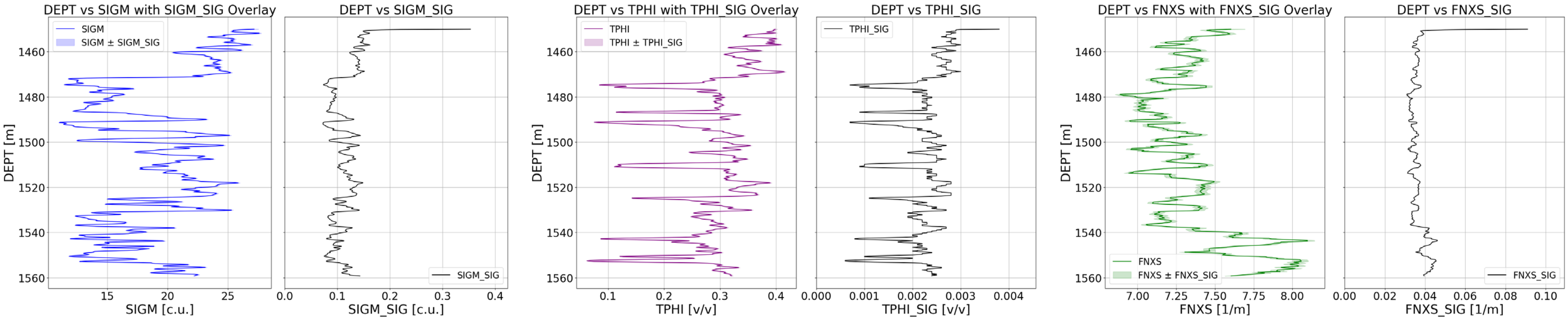

Coefficient of Variation of GSH-measurements

Key observations:

- ❑ High consistency and very good repeatability observed for GSH measurements across all passes

Eccentered configuration

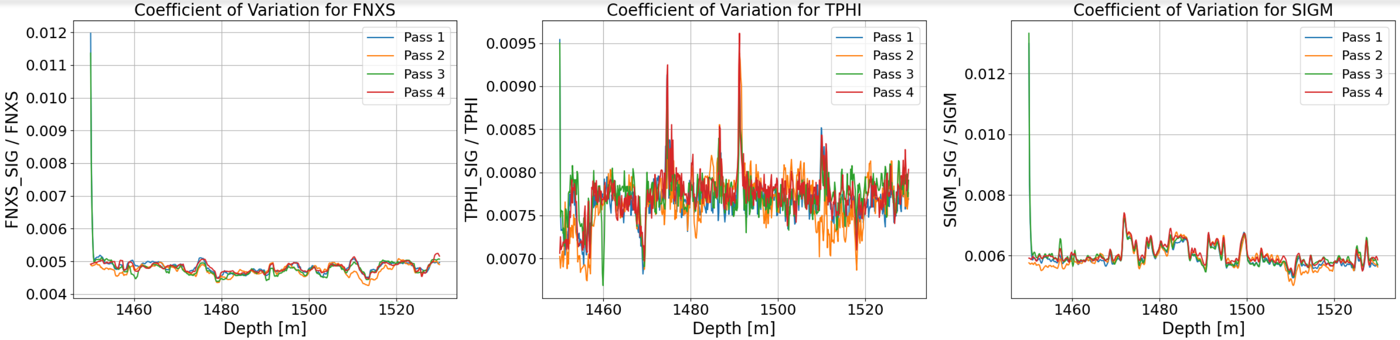

Centered configuration

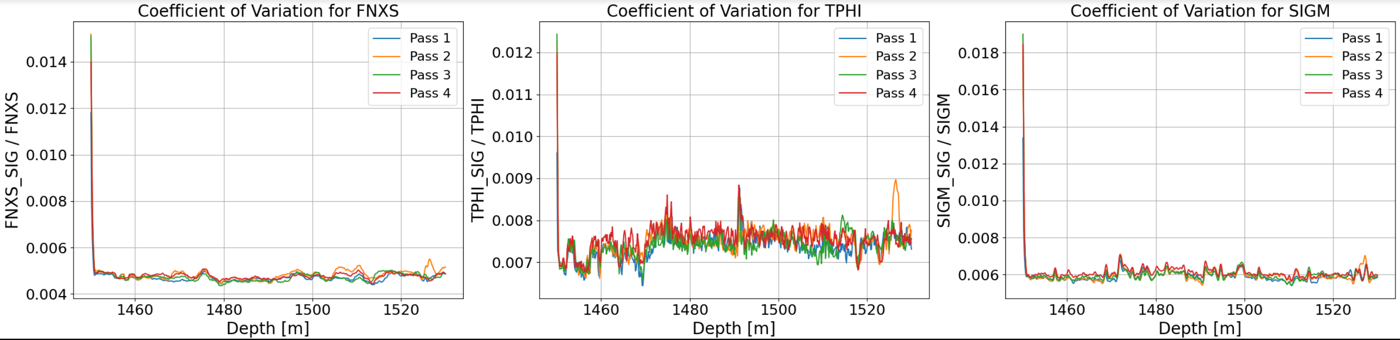

Acquisition of Monitoring logs

- Monitoring logs are being recorded daily in CRC-8
- Eccentered configuration has been chosen for the monitoring runs
- As of November 16, no CO_2 breakthrough has been observed on PNX logs
- Expected behavior to monitor in the logs in the presence of gas/sc-liquid:
  - FNXS (highly sensitive to gas): is expected to decrease
  - TPHI (highly sensitive to gas): is also expected to decrease
  - SIGM (less sensitive to gas): may or may not show significant statistical variation
  - Mineral mass fractions: expected to remain unchanged in siliciclastic environment for the duration of experiment

Monitoring log – Nov 16

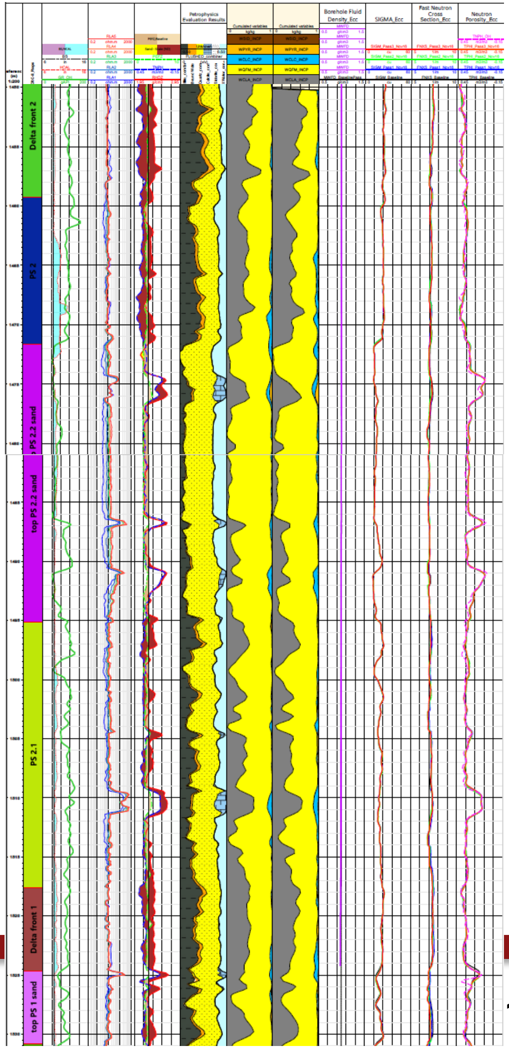

Upcoming milestones and Future Work

- Confirm the presence of CO_2 breakthrough during the primary drainage phase
- Identify and quantify the saturation of CH_4 and CO_2 components in the Buttress gas mixture
- Natural imbibition will occur during the post-injection period, which will lead to increase in water saturation
- Create a high-resolution lithofacies model corresponding to CRC-8 using a combination of well logs, FMI data, QEMSCAN data, and micro-CT images of cores

Thank you!

Novel Physics-based Method for Enhancement of Log Resolution

Step 1: Acquisition of low-resolution PN-logs

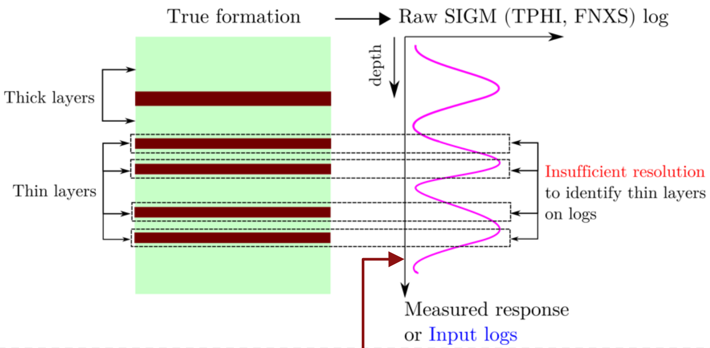

Compare logs

Step 2: Mathematical formulation of the target problem

Step 2(a): Defining the objective function

$$b(i) = \int_{z=i-\frac{1}{2}VR}^{i+\frac{1}{2}VR} w_{iz} \cdot x(z)\, dz \approx \sum_{z=i-\frac{1}{2}VR}^{i+\frac{1}{2}VR} w_{iz} \cdot x(z) \cdot \Delta z$$

$b(i)$ log values at sampled depth i

w_{iz} weight coefficients at sampled depth i over the depth of investigation

$x(z)$ real (or in-situ) properties of layer at depth z

VR vertical resolution of the PNL tool

Step 2(b): Physics-based constraints

Using the well-log interpretation model, the upper and lower bounds of measured properties, such as porosity, SIGM, etc., are computed interactively

Step 2(c): Deterministic optimization problem

$$x'_{high-res} = argmin_{high-res}(b(i) - sim(i))^2$$

given constraints

Algorithm: Constrained least squares method

Step 3: Data Assimilation

- The sliding window technique is employed to obtain a sufficient number of equations
- This method simulates the operating state of the tool, as the current tool sampling includes overlapping formation information from previous samplings

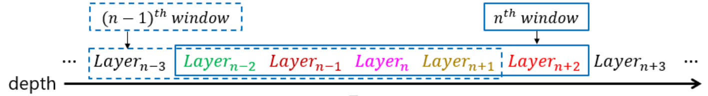

transform to equations

$$\begin{array}{c} \\ \\ \\ n^{th}\ window\ equation \\ \\ \end{array} \begin{bmatrix} w_{11}x_1 + w_{12}x_2 + w_{13}x_3 + w_{14}x_4 + w_{15}x_5 \\ w_{22}x_2 + w_{23}x_3 + w_{24}x_4 + w_{25}x_5 + w_{26}x_6 \\ \cdots \\ w_{i(n-2)}x_{n-2} + w_{i(n-1)}x_{n-1} + w_{i(n)}x_n + w_{i(n+1)}x_{(n+1)} + w_{i(n+2)}x_{n+2} \\ \cdots \end{bmatrix} = \begin{bmatrix} b(3) \\ b(4) \\ \cdots \\ b(n) \\ \cdots \end{bmatrix}$$

Step 4: Output high-resolution PN-logs

- The solution to the optimization problem results in estimation of the true profile of the formation with enhanced resolution

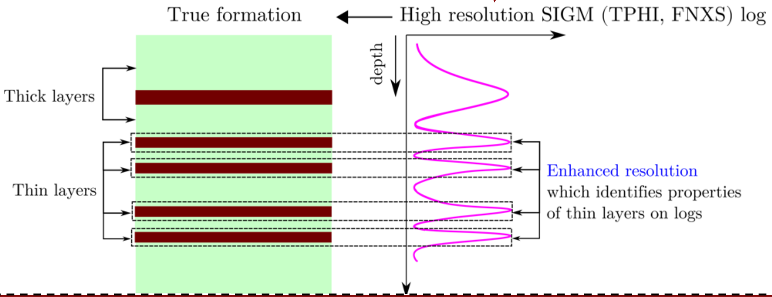

Scaled-D for SIGM

Key observations:

- Excellent repeatability observed for SIGM across all pairs of passes in both eccentered and centered configurations, with the Scaled-D ratio consistently between $\pm 5\%$
- A few outliers were mostly observed near the boundary between the top PS1 sand and PS 1.2 formations

Eccentered configuration

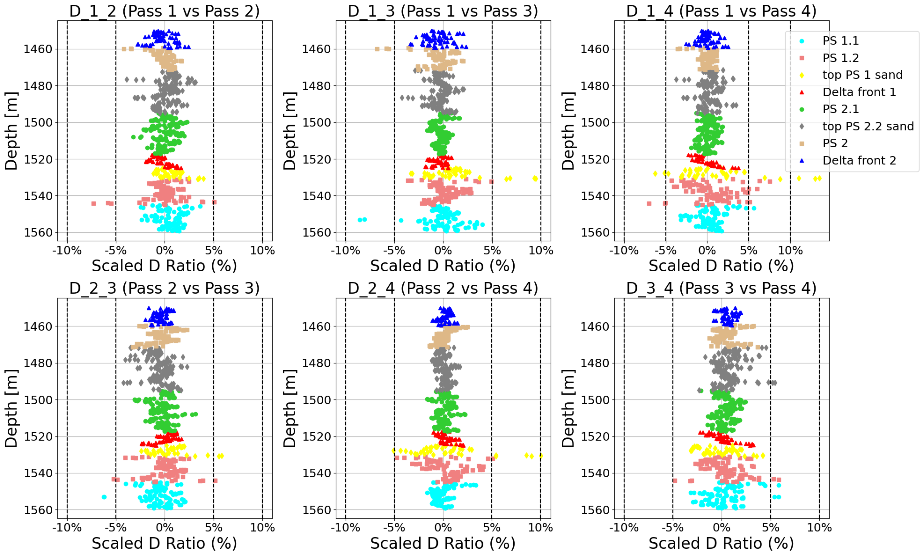

Centered configuration

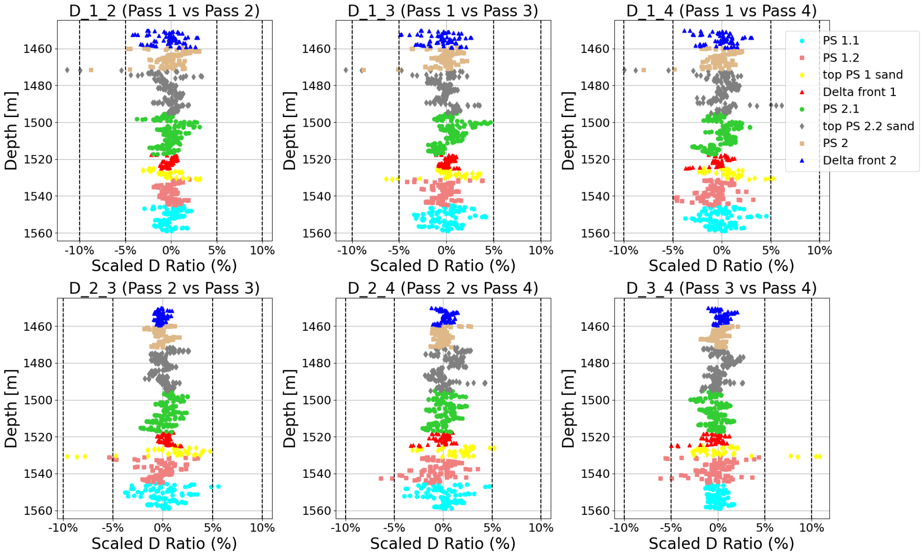

Scaled-D for TPHI

Key observations:

- Good repeatability observed for TPHI across all pairs of passes in both configurations
- Significant deviations were primarily observed in the PS 1.1 formation, where the likelihood of plume arrival is low

Eccentered configuration

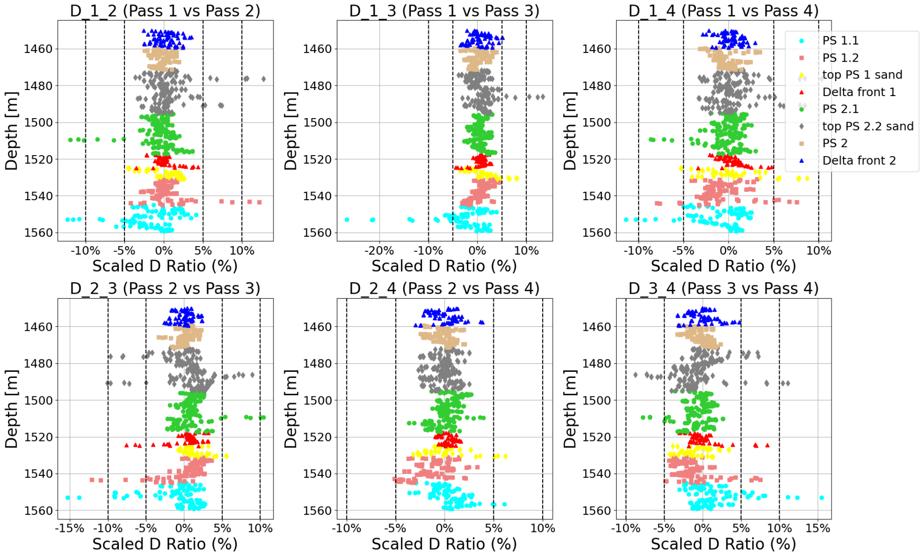

Centered configuration

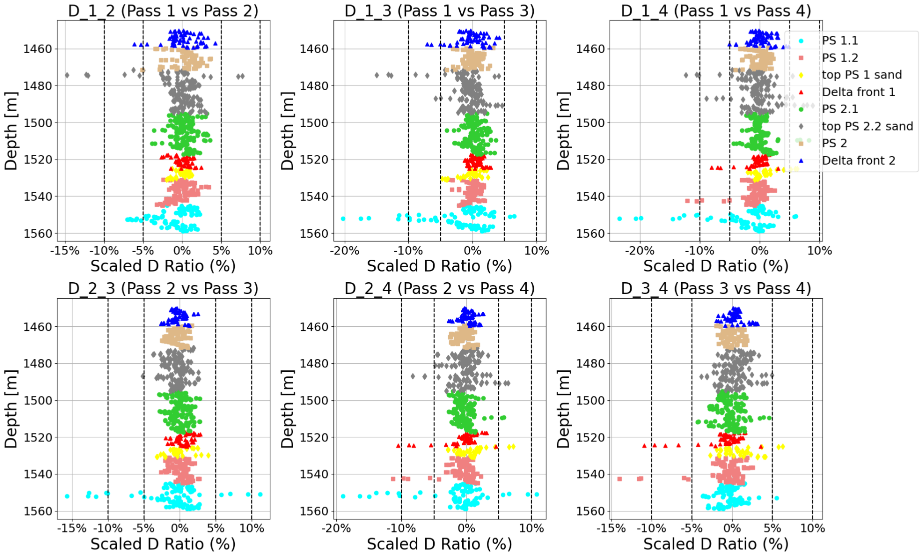

Scaled-D for FNXS

Key observations:

- Excellent repeatability observed for FNXS across all pairs of passes in both configurations
- Due to this high repeatability, the eccentered configuration was selected for the monitoring runs of the GFV experiment

Eccentered configuration

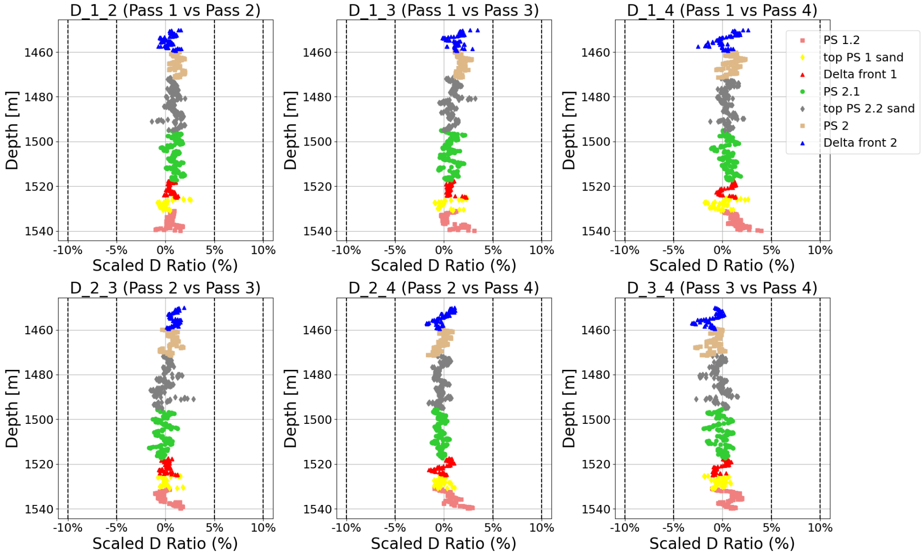

Centered configuration